Boundary-Layer Meteorol (2016) 158:351–359
DOI 10.1007/s10546-015-0089-6

NOTES AND COMMENTS

Radon as an Indicator of Nocturnal Atmospheric Stability: A Simplified Theoretical Approach

Yasutaka Omori[1] · **Hiroyuki Nagahama**[2]

Received: 8 October 2014 / Accepted: 8 September 2015 / Published online: 26 September 2015

Abstract Nocturnal evolution of radon concentration and the height of a box model, which is determined from radon concentration and local radon flux at the ground, are used as indicators of nocturnal atmospheric stability in single-height observations. However, quantitative relationships between these indicators and meteorological conditions, including the turbulent diffusion coefficient, have not yet been well established. Here, we construct a simple model based on the heat exchange process of the lower atmosphere to relate these parameters. The model neglects radiative flux divergence and assumes a uniform constant radon flux, making it most applicable to low wind conditions at sites well-removed from coastal influences, when advective effects are minimal. The model shows that the box height (equivalent mixing height) can be determined from near-surface parameters including sensible heat flux and the decrease in potential temperature after sunset. For these parameters, static stability and mechanical mixing components are incorporated. In addition, the constructed equations suggest the equivalent mixing height is proportional to the inversion layer height with a slope that depends on the vertical profile of potential temperature. The equivalent mixing height can be also related to the turbulent diffusion intensity. We demonstrate that radon observations at a single height are useful for monitoring nocturnal atmospheric stability.

Keywords Equivalent mixing height · Inversion layer · Radon · Sensible heat flux · Turbulent diffusion

1 Introduction

Radon-222 (radon) is a radionuclide that has been widely used for investigating vertical mixing in the atmospheric boundary layer (e.g. Jacobi and André 1963; Liu et al. 1984;

✉ Yasutaka Omori
ys-omori@fmu.ac.jp

1 Department of Radiation Physics and Chemistry, Fukushima Medical University, 1 Hikarigaoka, Fukushima, Fukushima 960-1295, Japan

2 Department of Geoenvironmental Sciences, Graduate School of Science, Tohoku University, 6-3 Aramaki-Aza-Aoba, Aoba-ku, Sendai 980-8578, Japan

Butterweck et al. 1994; Desideri et al. 2006; Williams et al. 2011), because its half-life (3.8 days) is long compared to typical turbulent time scales (1 h or less) in the atmospheric boundary layer and production and removal processes are simple. Radon is a radioactive noble gas produced from Ra-226, which is abundant in rocks and soils. Radon flux from unsaturated land surfaces is so much larger than the flux from the ocean surface that its source is regarded as solely continental (Wilkening and Clements 1975; Schery and Wasiolek 1998). Once exhaled into the atmosphere, radon is transported by turbulent diffusion without chemical reaction or deposition, and it is unlikely to be washed out by rainfall. Consequently, it is eliminated predominantly by the radioactive decay process (Porstendörfer 1994; Zahorowski et al. 2004).

Several studies have related vertical radon profiles to the strength of atmospheric stability or turbulent diffusion based on multi-height observations (e.g. Moses et al. 1960; Hosler 1969; Liu et al. 1984; Williams et al. 2011, 2013; Chambers et al. 2011; Kondo et al. 2014; Vargas et al. 2015). On the other hand, the nocturnal evolution of radon (i.e. radon gradient) in time series obtained at a near-surface single level is also a good indicator of vertical mixing (e.g. Perrino et al. 2001; Chambers et al. 2015a, b). Chambers et al. (2015a, b) showed that trends in air pollutant concentrations were separated more clearly using atmospheric stability based on the radon gradient than the Pasquill–Gifford stability classification. Another indicator is the height of a box model that is related to the radon gradient (e.g. Fontan et al. 1979; Guedalia et al. 1980; Fujinami and Esaka 1988; Allegrini et al. 1994; Kataoka et al. 1998; Sesana et al. 1998; Galmarini 2006; Griffiths et al. 2013; Chambers et al. 2015b). For investigating nocturnal atmospheric stability, Guedalia et al. (1980) introduced the following simplified equation,

$$h_{\mathrm{e}}(t) = \frac{E}{C(t) - C(0)} t, \tag{1}$$

where E is the local radon flux at the earth's surface, t is the collapse time from initiation of radon accumulation, and $C(t)$ and $C(0)$ are radon concentrations at time t and the initial time, respectively. The box height $h_{\mathrm{e}}(t)$, which is called the equivalent mixing height, is several tens of m in magnitude in the stable nocturnal boundary layer (e.g. Fontan et al. 1979; Sesana et al. 1998, 2003, 2006; Chambers et al. 2015b). However, it has not been clarified how both the radon gradient and h_{e} are related to meteorological conditions. In addition, although h_{e} agrees well with the mixing depth in the convective boundary layer during daytime (Fujinami and Esaka 1988; Kataoka et al. 1998), a definitive relationship between h_{e} and the inversion layer height h_{i} at night has yet to be established.

In the present paper, we provide approximate means for relating the radon gradient and h_{e} to (1) meteorological conditions, (2) inversion layer height, and (3) turbulent diffusion using single-height observations for estimating nocturnal atmospheric stability.

2 Nocturnal Evolution of Radon Concentrations with Inversion Layer Development

Around late afternoon, the surface heat flux becomes negative (from the surface upward), and a nocturnal inversion layer, which has a positive potential temperature gradient, gradually forms from the surface upward (Stull 1988). The sensible heat flux $H(t)$ is expressed by

$$H(t) = -\rho C_{\mathrm{p}} K_{\mathrm{H}}(z, t) \frac{\partial \theta(z, t)}{\partial z}, \tag{2}$$

where $K_H(z, t)$ is the turbulent diffusion coefficient for heat, $\theta(z, t)$ is the potential temperature, ρ is the air density, C_p is the specific heat of air, and z is the height (Li 1974; Stull 1988; Arya 2001). When, at the inversion layer height, the potential temperature is equal to that at ground level at the initial time and its gradient is zero (Fig. 1), the inversion layer height $h_i(t)$ is determined from

$$h_i(t) = \frac{H_{av}(t)}{\alpha \rho C_p \left[\theta(0, t) - \theta(0, 0)\right]} t, \tag{3}$$

where, $H_{av}(t)$ is the average sensible heat flux from time 0 to t, and α is a constant that depends on the vertical distribution of potential temperature (for a linear distribution, $\alpha = 0.5$) (Stull 1988; Betts 2006).

Under weakly stable to very stable nocturnal conditions, there is a well-defined evolution of radon concentration near the surface due to the suppression of radon dispersion and continuous radon emission (Moses et al. 1960; Porstendörfer 1994; Dueñas et al. 1996; Omori et al. 2009). The radon flux $E(t)$ follows Fick's law and is given by

$$E(t) = -K_R(z, t) \frac{\partial C(z, t)}{\partial z}, \tag{4}$$

where $K_R(z, t)$ is the turbulent diffusion coefficient of radon and $C(z, t)$ is the radon concentration (Li 1974; Fleischer 1980; Dueñas et al. 1997). Combining Eq. 2 with Eq. 4, we can relate the variation of the radon concentration to thermodynamic processes in the atmosphere. When $K_H(z, t) = K_R(z, t)$ is considered (e.g. Anquetin et al. 1999; Vinod Kumar et al. 1999; Olivié et al. 2004), then

$$\frac{\partial C(z, t)}{\partial z} = \frac{\rho C_p E(t)}{H(t)} \frac{\partial \theta(z, t)}{\partial z}, \tag{5}$$

and integration of Eq. 5 from the surface to altitude z at time t gives

$$C(z, t) - C(0, t) = \frac{\rho C_p E(t)}{H(t)} \left[\theta(z, t) - \theta(0, t)\right]. \tag{6}$$

Equation 6 implies that the vertical distribution of radon is characterized by that of potential temperature and the turbulent heat flux (see also Li 1974). It is worthwhile noting that a similar relation can also be obtained via dimensional analysis using the Buckingham Pi theorem (Buckingham 1914, see Appendix 1).

The relationship in Eq. 6 can be transformed into a relationship between a time series of radon concentrations and potential temperature at the surface (even though this is an impractical height at which to observe radon). In the following discussion, the radioactive decay of radon is ignored at the nocturnal time scale (e.g. Allegrini et al. 1994; Betts 2006; Chambers et al. 2011; Williams et al. 2013). Let us consider a situation when heat flux changes from positive to negative and atmospheric stability is neutral at time $t = 0$. According to Eq. 6, since $\theta(z, 0) = \theta(0, 0)$ (Fig. 1), the vertical distribution of radon concentration is also constant: $C(z, 0) = C(0, 0)$. Next, we consider the situation when atmospheric cooling proceeds and the inversion layer reaches $z = h_i$ at t. The potential temperature at h_i is equal to that at $z = 0$ and $t = 0$, i.e. $\theta(h_i, t) = \theta(0, 0)$ (Fig. 1), which leads to $C(h_i, t) = C(0, 0)$. Then, based on these relationships, Eq. 6 can be transformed as follows,

$$C(0, 0) - C(0, t) = \frac{\rho C_p E(t)}{H(t)} \left[\theta(0, 0) - \theta(0, t)\right]. \tag{7}$$

Equation 7 indicates that the nocturnal radon gradient in a time series is quantified by the radon and sensible heat fluxes and the decrease in potential temperature. It is also shown

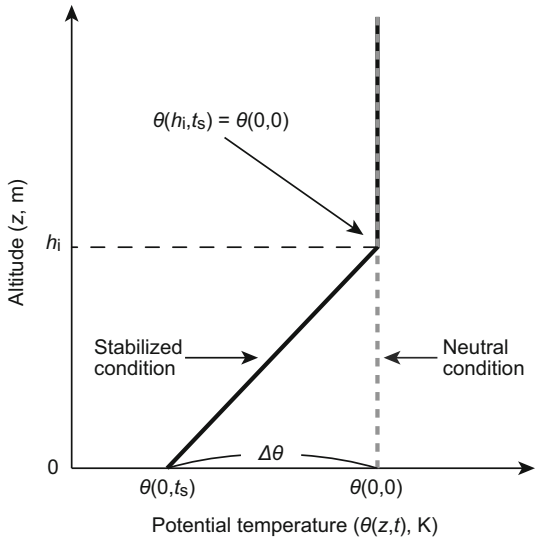

Fig. 1 Schematic representation of vertical profiles of potential temperature in the atmospheric boundary layer. This figure is drawn for a linear profile of potential temperature, i.e. $\alpha = 0.5$ in Eq. 3. *Grey broken and black solid lines* mean the vertical profile under neutral and stabilized conditions, respectively. The symbol h_i is the inversion layer height and t_s is the collapse time after sunset ($t = 0$)

that the local radon flux can be determined from the radon concentration and meteorological data.

The strength of atmospheric stability is related to the vertical temperature gradient and the wind-speed gradient (Stull 1988; Chambers et al. 2011; Williams et al. 2013). In Eq. 7, the static stability and the mechanical mixing components are incorporated into the potential temperature change and sensible heat flux, respectively. This is the reason why the radon gradient in a time series or equivalent mixing height can be regarded as a good indicator of nocturnal atmospheric stability.

3 Relationship Between Radon, Equivalent Mixing Height, Inversion Layer Height, and Turbulent Diffusion

The indicator of atmospheric stability h_e evaluated from radon concentrations can be connected to h_i since both radon concentrations and h_i follow the change of near-surface potential temperature. Combining Eq. 1 with Eq. 3 through Eq. 7, we obtain the following equation that shows a linear relationship between h_e and h_i,

$$h_\mathrm{e}(t) = \frac{\alpha H(t)}{H_\mathrm{av}(t)} h_\mathrm{i}(t), \tag{8}$$

which reveals that the slope of h_e against h_i depends on the nocturnal evolution of the sensible heat flux and the vertical distribution of the potential temperature. Under clear-sky conditions, the sensible heat flux tends to fluctuate less during the nocturnal period (e.g. Hicks 1981; Edwards et al. 2006), and therefore, $H(t) \approx H_\mathrm{av}(t)$ is assumed. Under this condition, Eq. 8 can be approximately written as

$$h_\mathrm{e}(t) \approx \alpha h_\mathrm{i}(t), \tag{9}$$

and indicating that the slope depends slightly on the heat flux, but primarily on α, the structure constant of the potential temperature profile.

This finding may be supported by the h_e and h_i data described in Allegrini et al. (1994), who calculated h_e from radon concentrations and inferred h_i from radiosonde data in Milan, Italy under weakly stable (summer) and moderately to strongly stable (winter) conditions, when horizontal advection can be ignored. Here, it should be noted that the urban mixing height used in Allegrini et al. (1994) is equivalent to h_i during a nocturnal period. They found that h_e is positively correlated with h_i. In addition, although the authors themselves considered that the magnitude of the slope was not statistically determined, the slope appeared to be about 0.5. Moreover, the slope was nearly constant regardless of the season, summer or winter. These findings imply that Eq. 8 (or its approximation Eq. 9) is useful for estimating h_e.

We now discuss the relationship between equivalent mixing height and turbulent diffusion intensity. According to Eqs. 2, 3, 8, and 9 assuming $K_H = K_R = K$, the relationship is satisfied, with

$$h_e^2(t) = \frac{\alpha H(t)}{H_{av}(t)} Kt \approx \alpha Kt, \tag{10}$$

or, as a function of h_i,

$$h_i^2(t) = \frac{H_{av}(t)}{\alpha H(t)} Kt \approx \frac{K}{\alpha} t. \tag{11}$$

The form of Eq. 10 is similar to that in Fontan et al. (1979), but the coefficient α in our equation is smaller ($\alpha = 0.8$ in Fontan et al. (1979)). This might be due to the difference in the derivation process, i.e., the former is derived mainly from thermodynamics (Eqs. 2, 3), while the latter is derived from Eqs. 1 and 4 with simplifications for h_e and the radon flux.

The turbulent diffusion coefficient typically has values $\sim 10^{-2}$–10 m^2 s^{-1} in the stabilized atmosphere as noted in Jacob (1999). In several previous studies using vertical radon profiles, Hosler (1969) obtained bulk turbulent diffusion coefficients ranging from 0.6 to 4.8 m^2 s^{-1} within a height of 90 m in nearly neutral to moderately stable conditions, while Chambers et al. (2011) estimated the bulk turbulent diffusion coefficients to be 0.12–0.44 m^2 s^{-1} within a height of 50 m in relatively stable conditions. In Kondo et al. (2014) and Vargas et al. (2015), the turbulent diffusion coefficient within a height of 100 m was at most 0.13 ± 0.05 m^2 s^{-1} in strongly stable conditions and 0.2–1.2 m^2 s^{-1} at lower wind speeds (< 5 m s^{-1}). Based on Eqs. 1 and 10 used in the present study and time series of near-surface radon concentrations and radon flux presented in Kondo et al. (2014) and Vargas et al. (2015), the diffusion coefficient and equivalent mixing height are estimated to be 0.09–0.20 m^2 s^{-1} and 30–60 m (radon gradient: 2.2–2.5 Bq m^{-3}, collapse time: 5–10 h), respectively, for Kondo et al. (2014), with the corresponding values of 0.2–1.5 m^2 s^{-1} and 30–50 m (radon gradient: 1.3–4.7 Bq m^{-3}, collapse time: 5–10 h) for Vargas et al. (2015). The estimated diffusion is very close to the observed values. In particular, a high similarity was obtained even when radiative cooling was not negligible (Kondo et al. 2014). The equivalent mixing height was also comparable to that reported in Chambers et al. (2015b) for moderately to strongly stable conditions (30–50 m). However, our estimations (K: 0.8–0.9 m^2 s^{-1}, h_e: 120 m) do not match the radon data (radon gradient: 2.0–2.4 Bq m^{-3}, collapse time: 8–10 h) reported in Chambers et al. (2011). This may be due to the topographic characteristic of the measurement site, which was located atop a broad ridge with significant slopes.

Finally, we now discuss the conditions under which the constructed equations can be applied. Time scales for absolute radon concentrations are composed of short (diurnal) and

long time scales (≥synoptic), with the advective (long time scale) contribution depending on the airmass fetch history over the past two weeks (e.g. Chambers et al. 2011, 2015b). However, in the model, radon is sourced locally, i.e. advective contribution is ignored throughout the course of a night. This assumption is thought to be valid since during stable nights, when wind speeds are low, most observed radon is contributed to for fetches within a radius of approximately several tens of km (Sakashita et al. 1996; Chambers et al. 2011). In addition, the model is not, in principle, applicable to coastal regions due to the presence of large differences in radon flux between onshore and offshore areas. In the absence of rainfall, which leads to an increase in soil moisture and subsequent reduction in radon flux (e.g. Stranden et al. 1984; Hosoda et al. 2007), the radon flux is considered to be nearly constant throughout a night. In addition, for the formulation, meteorological conditions such as the presence of clear skies and the absence of radiative cooling are idealized. Nocturnal cloud cover affects net longwave radiation and, if winds are weak, the radiative flux divergence is not negligible. When the radiative flux divergence is dominant, the potential temperature profile has a negative curvature without affecting radon concentrations (e.g. André and Mahrt 1982; Duynkerke 1999; Ha and Mahrt 2003), and a linear profile of potential temperature can no longer be assumed. With regard to these limitations, however, it is noted that valid estimates were obtained for observations of a coastal site as shown in Vargas et al. (2015) and under conditions where radiative cooling was not negligible, as reported by Kondo et al. (2014). Available radon and meteorological data are limited and should be the subject of future work.

4 Conclusions

We have provided a simple model to show that nocturnal radon evolution and equivalent mixing height (box height) are good indicators of atmospheric stability. Under conditions of constant local radon flux, air density, and heat capacity of air and ignoring advective contributions to changes in radon concentration and radiative cooling, the nocturnal evolution of radon concentrations can be expressed as a function of only two variables, sensible heat flux and decrease in potential temperature (≈ air temperature) near the surface. Based on our model, the equivalent mixing height has a linear relationship with the inversion layer height, with a slope that depends primarily on the vertical distribution of potential temperature under the condition of small variations in sensible heat flux. In addition, the equivalent mixing height can be related to the turbulent diffusion coefficient. These results indicate that radon observations at a single height are useful for monitoring nocturnal atmospheric stability.

Acknowledgments We would like to thank the reviewers for their valuable comments. Part of this work was financially supported by the JSPS Research Fellowship for Young Scientists (Y. Omori).

Appendix 1

Dimension analysis using the Pi theorem (Buckingham 1914) is applied to a system governing the variation of radon concentration through heat exchange in a layer. An air layer with two parallel surfaces at a distance of Δz is considered where the lower and the upper surfaces correspond to the ground and inversion layer height in the environment, respectively. The whole layer is characterized by the density ρ and the specific heat C_p of air. In addition, radon and heat are supplied to the layer only at the lower surface and their rates are expressed as

Table 1 List of physical quantities with dimensions governing the variation of radon concentration through heat exchange in a system

Physical quantity	Symbol	Dimension (M, L, S, V, T, K)
Thickness of a layer	Δz	(0, 1, 0, 0, 0, 0)
Vertical gradient of radon concentration	$\Delta C(\Delta z, t)/\Delta z$	(0, −1, 0, −1, −1, 0)
	$(\Delta C(\Delta z, t) = C(\Delta z, t) - C(0, t))$	
Radon flux	$E(t)$	(0, 0, −1, 0, −2, 0)
Vertical gradient of air temperature	$\Delta\theta(\Delta z, t)/\Delta z$	(0, −1, 0, 0, 0, 1)
	$(\Delta\theta(\Delta z, t) = \theta(\Delta z, t) - \theta(0, t))$	
Sensible heat flux	$H(t)$	(1, 0, 0, 0, −3, 0)
Air density	ρ	(1, 0, 0, −1, 0, 0)
Specific heat of air	C_p	(0, 0, 1, 0, −2, −1)

$E(t)$ and $H(t)$, respectively. Under these conditions, we investigate the relationship between vertical gradients of radon concentration $\Delta C(\Delta z, t)/\Delta z(\Delta C(\Delta z, t) = C(\Delta z, t) - C(0, t))$ and potential temperature $\Delta\theta(\Delta z, t)/\Delta z(\Delta\theta(\Delta z, t) = \theta(\Delta z, t) - \theta(0, t))$. Table 1 lists the fundamental dimensions of seven physical quantities in the considered system. In this study, we identify six fundamental dimensions: mass (M), length (L), area (S), volume (V), time (T), and temperature (K), although area and volume scales may be converted into the length dimension in ordinary studies. Based on these quantities, we may construct the functional relation in dimensional form: $f(\Delta C(\Delta z, t)/\Delta z, \Delta\theta(\Delta z, t)/\Delta z, E(t), H(t), \rho, C_\mathrm{p}, \Delta z) = 0$. Based on the Pi theorem, only one dimensionless product is determined and, therefore, the following dimensionless expression is given as

$$\phi\left(\frac{H(t)\frac{\Delta C(\Delta z,t)}{\Delta z}\Delta z}{\rho C_\mathrm{p} E(t)\frac{\Delta\theta(\Delta z,t)}{\Delta z}\Delta z}\right) = 0, \tag{12}$$

or

$$\frac{H(t)\Delta C(\Delta z, t)}{\rho C_p E(t)\Delta\theta(\Delta z, t)} = A, \tag{13}$$

where A is a constant. We assume from the discussions in Sect. 2 that the dimensionless constant A represents the ratio of the turbulent diffusion coefficient of heat (K_H) to the turbulent diffusion coefficient of radon (K_R). For $A = 1$, the linear relationship between radon concentration and potential temperature is obtained in a form similar to Eq. 6.

References

Allegrini I, Febo A, Pasini A, Schiarini S (1994) Monitoring of the nocturnal mixed layer by means of particulate radon progeny measurement. J Geophys Res 99(D9):18765–18777

André JC, Mahrt L (1982) The nocturnal surface inversion and influence of clear-air radiative cooling. J Atmos Sci 39:864–878

Anquetin S, Guilbaud C, Chollet J-P (1999) Thermal valley inversion impact on the dispersion of a passive pollutant in a complex mountainous area. Atmos Environ 33:3953–3959

Arya SP (2001) Introduction to micrometeorology, 2nd edn. Academic Press, San Diego 420 pp

Betts AK (2006) Radiative scaling of the nocturnal boundary layer and the diurnal temperature range. J Geophys Res 111:D07105. doi:10.1029/2005JD006560
Buckingham E (1914) On physically similar systems; illustrations of the use of dimensional equations. Phys Rev 4:345–376
Butterweck G, Reineking A, Kesten J, Porstendörfer J (1994) The use of the natural radioactive noble gases radon and thoron as tracers for the study of turbulent exchange in the atmospheric boundary layer - case study in and above a wheat field. Atmos Environ 28:1963–1969
Chambers S, Williams AG, Zahorowski W, Griffiths A, Crawford J (2011) Separating remote fetch and local mixing influences on vertical radon measurements in the lower atmosphere. Tellus 63B:843–859
Chambers SD, Wang F, Williams AG, Xiaodong D, Zhang H, Lonati G, Crawford J, Griffiths AD, Ianniello A, Allegrini I (2015a) Quantifying the influences of atmospheric stability on air pollution in Lanzhou, China, using a radon-based stability monitor. Atmos Environ 107:233–243
Chambers SD, Williams AG, Crawford J, Griffiths AD (2015b) On the use of radon for quantifying the effects of atmospheric stability on urban emissions. Atmos Chem Phys 15:1175–1190
Desideri D, Roselli C, Feduzi L, Assunta Meli M (2006) Monitoring the atmospheric stability by using radon concentration measurements: a study in a Central Italy site. J Radioanal Nucl Chem 270:523–530
Duynkerke PG (1999) Turbulence, radiation and fog in Dutch stable boundary layers. Boundary-layer Meteorol 90:447–477
Dueñas C, Pérez M, Fernández MC, Carretero J (1996) Radon concentrations in surface air and vertical atmospheric stability of the lower atmosphere. J Environ Radioact 31:87–102
Dueñas C, Fernández MC, Carretero J, Liger E, Pérez M (1997) Release of ^{222}Rn from some soils. Ann Geophys 15:124–133
Edwards JM, Beare RJ, Lapworth AJ (2006) Simulation of the observed evening transition and nocturnal boundary layers: single-column modelling. Q J R Meteorol Soc 132:61–80
Fleischer RL (1980) Radon flux from the earth: methods of measurement by the nuclear track technique. J Geophys Res 85(C12):7553–7556
Fontan J, Guedalia D, Druilhet A, Lopez A (1979) Une methode de mesure de la stabilite verticale de l'atmosphere pres du sol. Boundary-layer Meteorol 17:3–14 (in French, with English abstract)
Fujinami N, Esaka S (1988) A simple model for estimating the mixing depth from the diurnal variation of atmospheric ^{222}Rn concentration. Radiat Prot Dosim 24:89–91
Galmarini S (2006) One year of ^{222}Rn concentration in the atmospheric surface layer. Atmos Chem Phys 6:2865–2887
Griffiths AD, Parkes SD, Chambers SD, McCabe MF, Williams AG (2013) Improved mixing height monitoring through a combination of lidar and radon measurements. Atmos Meas Tech 6:207–218
Guedalia D, Ntsila A, Druilhet A, Fontan J (1980) Monitoring of the atmospheric stability above an urban and suburban site using sodar and radon measurements. J Appl Meteorol 19:839–848
Ha K-J, Mahrt L (2003) Radiative and turbulent fluxes in the nocturnal boundary layer. Tellus 55A:317–327
Hicks BB (1981) An analysis of Wangara micrometeorology: surface stress, sensible heat, evaporation, and dewfall. NOAA Technical Memorandum ERL ARL-104, 36 pp
Hosler CR (1969) Vertical diffusivity from radon profiles. J Geophys Res 74:7018–7026
Hosoda M, Shimo M, Sugino M, Furukawa M, Fukushi M (2007) Effect of soil moisture content on radon and thoron exhalation. J Nucl Sci Technol 44:664–672
Jacob DJ (1999) Introduction to atmospheric chemistry. Princeton University Press, Princeton 266 pp
Jacobi W, André K (1963) The vertical distribution of radon 222, radon 220 and their decay products in the atmosphere. J Geophys Res 68:3799–3814
Kataoka T, Yunoki E, Shimizu M, Mori T, Tsukamoto O, Ohhashi Y, Sahashi K, Maitani T, Miyashita K, Fujikawa Y, Kudo A (1998) Diurnal variation in radon concentration and mixing-layer depth. Boundary-layer Meteorol 89:225–250
Kondo H, Murayama S, Sawa Y, Ishijima K, Matsueda H, Wada A, Sugawara H, Onogi S (2014) Vertical diffusion coefficient under stable conditions estimated from variations in the near-surface radon concentration. J Meteorol Soc Jpn 92:95–106
Li T-Y (1974) Diurnal variations of radon and meteorological variables near the ground. Boundary-layer Meteorol 7:185–198
Liu SC, McAfee JR, Cicerone RJ (1984) Radon 222 and tropospheric vertical transport. J Geophys Res 89(D5):7291–7297
Moses H, Stehney AF, Lucas HF Jr (1960) The effect of meteorological variables upon the vertical and temporal distributions of atmospheric radon. J Geophys Res 65:1223–1238
Olivié DJL, van Velthoven PFJ, Beljaars ACM (2004) Evaluation of archived and off-line diagnosed vertical diffusion coefficients from ERA-40 with ^{222}Rn simulations. Atmos Chem Phys 4:2313–2336

Omori Y, Tohbo I, Nagahama H, Ishikawa Y, Takahashi M, Sato H, Sekine T (2009) Variation of atmospheric radon concentration with bimodal seasonality. Radiat Meas 44:1045–1050

Perrino C, Pietrodangelo A, Febo A (2001) An atmospheric stability index based on radon progeny measurements for the evaluation of primary urban pollution. Atmos Environ 35:5235–5244

Porstendörfer J (1994) Properties and behaviour of radon and thoron and their decay products in the air. J Aerosol Sci 25:219–263

Sakashita T, Murakami T, Iida T, Ikebe Y, Chino M, Suzuki K (1996) Simulation of diurnal variation of atmospheric ^{222}Rn concentrations with three-dimensional atmospheric dispersion model. Jpn J Health Phys 31:161–168 (in Japanese with English abstract)

Schery SD, Wasiolek MA (1998) Modeling radon flux from the earth's surface. In: Katase A, Shimo M (eds) Radon and thoron in the human environment, proceedings of the 7th Tohwa University International Symposium. World Scientific Publishing Company, Singapore, pp 207–217

Sesana L, Barbieri L, Facchini U, Marcazzan G (1998) ^{222}Rn as a tracer of atmospheric motions: a study in Milan. Radiat Prot Dosim 78:65–71

Sesana L, Caprioli E, Marcazzan GM (2003) Long period study of outdoor radon concentration in Milan and correlation between its temporal variations and dispersion properties of atmosphere. J Environ Radioact 65:147–160

Sesana L, Ottobrini B, Polla G, Facchini U (2006) ^{222}Rn as indicator of atmospheric turbulence: measurements at Lake Maggiore and on the pre-Alps. J Environ Radioact 86:271–288

Stranden E, Kolstad AK, Lind B (1984) The influence of moisture and temperature on radon exhalation. Radiat Prot Dosim 7:55–58

Stull RB (1988) An introduction to boundary layer meteorology. Kluwer Academic Publishers, Dordrecht 666 pp

Vargas A, Arnold D, Adame JA, Grossi C, Hernández-Ceballos MA, Bolivar JP (2015) Analysis of the vertical radon structure at the Spanish "El Arenosillo" tower station. J Environ Radioact 139:1–17

Vinod Kumar A, Sitaraman V, Oza RB, Krishnamoorthy TM (1999) Application of a numerical model for the planetary boundary layer to the vertical distribution of radon and its daughter products. Atmos Environ 33:4717–4726

Wilkening MH, Clements WE (1975) Radon 222 from the ocean surface. J Geophys Res 80:3828–3830

Williams AG, Zahorowski W, Chambers S, Griffiths A, Hacker JM, Element A, Werczynski S (2011) The vertical distribution of radon in clear and cloudy daytime terrestrial boundary layers. J Atmos Sci 68:155–174

Williams AG, Chambers S, Griffiths A (2013) Bulk mixing and decoupling of the nocturnal stable boundary layer characterized using a ubiquitous natural tracer. Boundary-layer Meteorol 149:381–402

Zahorowski W, Chambers SD, Henderson-Sellers A (2004) Ground based radon-222 observations and their application to atmospheric studies. J Environ Radioact 76:3–33